Mapping Functional Connectivity in the Rodent Brain Using Electric-Stimulation fMRI

Laura Pérez-Cervera, José María Caramés, Luis Miguel Fernández-Mollá, Andrea Moreno, Begoña Fernández, Elena Pérez-Montoyo, David Moratal, Santiago Canals, and Jesús Pacheco-Torres

Abstract

Since its discovery in the early 90s, BOLD signal-based functional Magnetic Resonance Imaging (fMRI) has become a fundamental technique for the study of brain activity in basic and clinical research. Functional MRI signals provide an indirect but robust and quantitative readout of brain activity through the tight coupling between cerebral blood flow and neuronal activation, the so-called neurovascular coupling. Combined with experimental techniques only available in animal models, such as intracerebral micro- stimulation, optogenetics or pharmacogenetics, provides a powerful framework to investigate the impact of specific circuit manipulations on overall brain dynamics. The purpose of this chapter is to provide a comprehensive protocol to measure brain activity using fMRI with intracerebral electric micro-stimulation in murine models. Preclinical research (especially in rodents) opens the door to very sophisticated and informative experiments, but at the same time imposes important constrains (i.e., anesthetics, translatability), some of which will be addressed here.

Key words fMRI, BOLD, Intracerebral micro-stimulation, Preclinical MRI

Preprint for academic book chapter in Preclinical MRI, Methods in Molecular Biology

1. Introduction

Neuroscience is currently one of the most challenging areas of biomedical research. The human brain and its function remain one of the last frontiers for modern science. Furthermore, there is a growing belief that its scientific understanding will have a pro- found effect on human progress, not only because of the improvement in treating neurologic and psychiatric disorders, but also because of the impact that a deep understanding of the brain would have on fields ranging from education, interpersonal relationships, the prolongation of a full physical and intellectual life and also for the development of a neuro-inspired Information and Communications Technology (ICT) society. In order to achieve this major goal, scientists need techniques that allow proper monitoring of brain function. Ideally, these techniques should satisfy the following criteria:

1. Applicable in vivo to study the intact brain.
2. To provide adequate temporal and spatial resolution.
3. To reflect the electrical activity of neurons as close as possible.
4. To be applicable in human and non-human animal models.

Over the past few decades, multiple non-invasive in vivo imaging methodologies have been developed to study brain function, although none of them has been able to fulfill all of the above mentioned criteria. These attempts can be classified on the basis of their strategies for measuring brain activity: directly assessing the electrical activity of the brain, or indirectly through surrogate measures as calcium transients, hemodynamic and/or metabolic changes associated to neuronal activity. Among the former we can include electroencephalography (EEG) and magnetoencephalography (MEG), which present excellent temporal resolution but have its particular Achilles' heel in the spatial resolution. The second category includes, among others, Positron Emission Tomography (PET) and Magnetic Resonance Imaging (MRI). Functional PET applications relay in the use of radioactively-labeled compounds metabolically active (15-Oxygen, 18F-Fluorodeoxyglucose.. .) whose measurement reports changes in blood flow, oxygen and/or glucose consumption, which are surrogates of neuronal activity. PET presents the highest sensitivity of all the afore mentioned

techniques, but the necessary use of radioactive com- pounds—with their short half-life and the relatively low spatial resolution—has hindered his widespread for neurological imaging purposes (see Ref. 1 for a review on neuroimaging techniques).

Functional magnetic resonance imaging (fMRI) utilizes MRI technology to indirectly measure brain activity by detecting changes associated with it. The best-known form of fMRI uses the blood-oxygen-level dependent (BOLD) contrast [2]. It relies on the brain's ability to locally modulate blood flow and volume to satisfy the increased energetic needs during neuronal activation. The relationship between increased local neural activity and changes in cerebral blood flow (CBF) is known as neurovascular coupling (or functional hyperemia). The correlation between BOLD signals and concomitantly recorded electrophysiological measures is well established [3, 4], although the exact molecular mechanism remains unclear [5] and its homogeneity throughout brain regions debated [4]. Functional MRI allows imaging brain activations with a spatial resolution as low as a few hundreds of microns (limited by the low intrinsic sensitivity of MRI, the small expected changes in signal intensity and the point spread function; for a review see [6]) and with a temporal resolution of seconds or even shorter (limited by the nature of the hemodynamic response itself).

It is important to stress that BOLD signals do not measure neuronal activity, but changes in neuronal activity (see [6] for a deeper discussion on the fundamentals of BOLD). Nevertheless, these changes in neuronal activity can occur spontaneously while the subject is not involved in any specific task. In those conditions the changes are of small amplitude and are referred to as resting state activity. Alternatively, the change in activity can be boosted by introducing a specific paradigm that defines an expected low activity state (baseline) and a high activity state (activation) that are subse- quently contrasted statistically. Common paradigms include the presentation of sensory stimuli, the introduction of a cognitive task, the administration of chemical substances, or the direct stimulation of the brain's parenchyma. In animal models, the availability of a larger repertoire of neuronal stimulation strategies allows the precise control of the stimulation parameters and neuronal populations being targeted. These

strategies include intracerebral direct electrical micro-stimulation and optogenetic or pharmacogenetic stimulation or inhibition of specific neuronal populations. These might overcome some of the limitations of sensory and task stimulation when the focus of the study is to unveil the precise neuronal circuits involved in a certain functional state. For instance, while activation of primary sensory structures is in some cases readily available by sensory stimulation, recruitment of other regions as some subcortical nuclei is more challenging. Also, the polysynaptic propagation of activity in intricate brain networks initiated by sensory stimuli or cognitive tasks makes it harder to investigate direct relationships or causality. Direct activation of a specific pathway or a neuronal population greatly eases such studies, allowing to investigate the consequences of precisely timed and accurately localized manipulation on the overall response of brain-wide networks.

Highly sophisticated and rich experiments can be done in animal models by the combination of fMRI with electrophysiological, optogenetic and pharmacogenetic tools. However, the use of animals (especially small animals as rats and mice) imposes certain limitations that need to be considered carefully. Spatial resolution issues, due to the smaller size of rodent's brains compared to primates, have been partially countervailed by the implementation of systems with ultrahigh magnetic fields and stronger radiofrequency gradients, yet still the obtained resolution is coarse for imaging certain subcortical structures. Therefore, partial volume effects need to be seriously considered. Also, the need for the absolute immobility of the subject during image acquisition has favored the used of anesthetized animals in most of the studies. Besides the obvious impact of anesthesia on neuronal activation, additional factors need to be considered in fMRI studies since anesthetics could directly impact on the hemodynamic response and the neurovascular coupling (discussed in detail in Subheading 3.1) [7] among other neuronal activation features. Some alternatives to avoid anesthetics are present, e.g., habituation training protocols which allow to do fMRI experiments in non-anesthetized rodents [8–10]. Although they are very appealing and pave the way to advance in rodent fMRI, the available protocols involve an initial period of severe stress during habituation to the MRI environment, which could interfere with the particular scientific

question at hand. Finally, further complications derived from the combination of fMRI with other recording or stimulation techniques include the need for MRI-compatible materials in all implants and devices required in the experiment.

The present protocol describes, stepwise, how to perform a BOLD fMRI experiment with intracerebral electric micro- stimulation, which has allowed us to (1) perform precise and con- trolled activations of selected brain regions, (2) reproducibly acquire data within and between animals in rats and mice, (3) to investigate the frequency-dependence of activity propagation in brain networks, and (4) to provide several insights into the synaptic plasticity control of long range connectivity.

2 Materials

2.1 Carbon Electrode Preparation

1. Theta-shaped glass capillary (World Precision Instruments, Florida, USA).
2. Carbon fibers.
3. Micropipette puller.
4. Bunsen burner.
5. Standard forceps, straight.
6. London forceps, angled.
7. Epoxy resin (fast drying).
8. Silver conductive epoxy resin.

2.2 Electrode Implantation Surgery

1. Isoflurane.
2. Urethane.
3. Bupivacaine.
4. Stereotaxic frame and stereotaxic micromanipulator.
5. Ophthalmic gel.
6. Heating pad with rectal thermal probe.
7. Surgical instruments:

(a) Small surgical scissors, straight.

(b) Standard forceps, straight.

(c) Dumont forceps, straight.

(d) Scalpel handle, straight.

(e) Non-sterile scalpel blade, curved, 22.

(f) Micro curette, straight.

(g) Micro drill trephine.

8. Sterile saline solution and hydrogen peroxide.

9. High-temperature Cautery kit.

10. Cotton.

11. Shaver.

12. Permanent marker.

13. 20G and 25G needles.

14. Tissue adhesive.

15. Bone acrylic.

16. Super-Bond C&B dental acrylic.

2.3 Functional MRI

The additional materials listed here are required to produce electri- cal brain stimulation in the rat while it remains in the magnet and acquire and process imaging data.

2.3.1 MRI Magnet

We use a horizontal 7 Tesla scanner with a 30 cm diameter bore (Biospec 70/30v, Bruker Medical, Ettlingen, Germany). The sys- tem has a 675 mT/m actively shielded gradient coil (Bruker, BGA 12-S) of 11.4 cm inner diameter. Data is acquired and pre-processed with a Hewlett-Packard console running Paravision 5.1 software (Bruker Medical GmbH, Ettlingen, Germany) operating on a Linux platform.

2.3.2 MRI Phase Array Coil

It is not indispensable, but it is highly convenient. The expected signal changes are in the range of 1–3% of the total signal intensity, thus it will

critically contribute to achieve the highest possible signal-to-noise ratio (SNR). We employ a1H rat brain receive-only phase array coil with integrated combiner and preamplifier, no tune/no match, in combination with the actively detuned transmit-only resonator (BrukerBioSpin MRI GmbH, Germany).

2.3.3 Physiological Monitoring and Control System

We use an MRI-compatible temperature control unit (MultiSens Signal conditioner, OpSens, Quebec, Canada). Other physiological parameters as heart rate (optimal values, 300 50 beats per min- ute), oxygen saturation (>95%), and breathing rate (90 10 breaths per minute) are monitored (see Note 1) throughout the session using an MRI-compatible sensor with foot clip (MouseOx, Starr Life Sciences, Oakmont, USA). Physiological parameters can be used to feed the analysis of BOLD signals (used as nuisance factors) which might be especially important in resting state experiments.

2.3.4 Heating System

It is crucial to keep the animal's temperature in the physiological range, and to maintain it stable (37 0.5 ◦C) in order to preserve vascular reactivity in response to neuronal activation. We use a water blanket connected to a water bath (Thermo Scientific SAHARA Heated Bath Circulators S5P) controlled by a temperature regulatory system (Thermo Scientific STANDARD Series Thermostats SC150) (see Note 2). In this system, precise control of the animal's temperature requires the constant attention of dedicated personnel to manually vary the temperature in the heating bath. In order to automate this process, a home-made and inexpensive closed loop regulation system has been developed to adjust water bath temperature to keep a constant body temperature in the animal (see details in Note 3).

2.3.5 Other Devices and Small Equipment

1. Pulse generator and current source (STG2004, Multichannel Systems, Reutlingen, Germany) for electric micro-stimulation.
2. Digital Oscilloscope to check electrode functionality.

3. Eye ointment (even if it is an acute procedure).

4. MRI-compatible stereotaxic device with ear- and bite-bars.

5. Agarose (0.5%) in saline. It is prepared and introduced in a 10cc syringe. It can be storage in the fridge before its use (see Note 4).

6. MRI sequences: gradient Echo (GE)-Echo Planar Imaging (EPI) sequence providing adequate temporal and spatial resolution (see Notes 5 and 6); and T2-weighted anatomical images, like a Rapid Acquisition Relaxation Enhanced (RARE) sequence (see Note 7).

2.3.6 Image Analysis Software

There are some commercially available software tools for fMRI analysis. In our case, fMRI data are analyzed offline using our own software developed in MatLab, which included Statistical Parametric Mapping package (SPM8, http://fil.ion.ucl.ac.uk/ spm), Analysis of Functional NeuroImages (AFNI, http://afni. nimh.nih.gov/afni), and FSL Software (FMRIB http://fsl.fmrib. ox.ac.uk/fsl).

2. Methods

All animal work should be carried out only upon review and approval of the methods by your institution's Animal Care and Use Committee [11, 12]. For those new to MRI and small animal surgery, prior to initiating any studies, training and advice should be sought from experts in the field.

Due to the presence of strong magnetic fields, surgery is performed in an area separated from the magnet room. Thus, it will be necessary to fix the stimulating and/or recording electrode to the animal's skull so that the animal can be safely transferred to the magnet room at the end of the surgery. Furthermore, due to the common use of surface coils in fMRI experiments, both the electrode positioning and its fixations must be done in such a way that allow maximal proximity between the MRI coil and the brain of the animal. Special care must be taken with bleeding during surgery, because any trace of blood will have a deep impact in the image quality, making it very difficult to obtain a reliable BOLD signal.

3.1 Anesthesia

As previously introduced, most fMRI experiments in rodents are performed in anesthetized animals. Different anesthetics have been introduced for fMRI studies in rodents, each of which presents its particular advantages and drawbacks (for a review see [7]) and all of them having an impact on the neurovascular coupling. At this point, it is important to emphasize that, in our experience, at least 80% of a successful fMRI experiment in rodents relies on maintain- ing the animal's physiology at adequate and steady-state values. Body temperature (37+/- 0.5 ◦C), oxygen saturation (>95%), CO2 (35–50 mmHg) and levels and blood pressure (130–140 mmHg) need to be fine-tuned. While precise monitoring of some of this values require invasive interventions (i.e., blood pressure and accurate CO2 measurements require femoral artery cannulation and tracheotomy, respectively) or direct blood sampling difficult to implement in longitudinal studies, pilot experiments with full monitoring of the animal's physiology are strongly recommended in setting up new anesthetic protocols.

The final election of an anesthetic method will depend on multiple factors like the species utilized (i.e., rats [13] vs. mice [14]), the duration of the experiment [15], whether it is an acute or longitudinal experiment, and even the type of stimuli used [16]. As a general rule, injectable anesthetics provide a stable imaging condition for up to 2 h, whereas inhaled anesthesia allows longer imaging sessions. An exception to this rule is urethane, which provides a stable and long-lasting (more than 8 h) anesthetized state with a single intraperitoneal injection and minimal cardiovascular effects [17]. Importantly, urethane also preserves most of the characteristic electrophysiological rhythms recorded in the hippocampus and other neocortical regions [18]. In the present protocol of electric stimulation fMRI, urethane has been the choice based on the above advantages [18]. However, urethane is restricted to terminal experiments due to its hepatotoxic and carcinogenic effects, for which it is compulsory to euthanize the animal at the end of the experiment. For chronic rat experiments and when working with mice, dexmedetomidine is the usual election [5]. It allows animal recovery but provides, in our hands, shorter periods of stable anesthesia (in the range of 1.5–2 h). An alternative administration regime for dexmedetomidine has been proposed to extend this period [19]. We have found significant

differences between different rats and mice strains. So we do recommend a pilot study in order to choose the most convenient anesthesia for each particular model.

3.2 Electric Stimulation

Stimulating electrodes dedicated to MRI experiments have been developed based on existing protocols [20]. Previous studies have shown the utility of iridium [21] or platinum-iridium electrodes [22] for this purpose. Nevertheless, these electrodes produce large susceptibility artifacts around the electrode's location, especially patent in EPI acquisition, precluding the possibility to study func- tional responses in the area close to the implant. To overcome this problem, we have introduced glass-coated carbon fiber bipolar electrodes in our setup, which present several advantages: most importantly the absence of susceptibility artifacts in the acquired brain images, but also the possibility to produce very thin bipolar electrodes (up to 7 μm tip diameter) [18].

To prepare carbon fiber electrodes, we use bundles of fibers inserted into a theta-shaped glass capillary previously pulled to form 7 mm long pipettes with 200 μm tip diameter and adjusted to produce an electrical impedance of 40–65 kΩ (see Note 8). A regular wire with a pin connector is attached to the pipette, connected to the carbon fibers using silver conductive epoxy resin, and isolated with clear epoxy resin [18].

Depending on the configuration used in the MRI, the glass electrode can be bent in order to accommodate the receiver coil, minimizing its distance to the brain and maximizing the signal-to- noise ratio (SNR) (see details in Subheading 3.4).

3.3 Stimulation Protocols

In previous work applying electric-stimulation fMRI to study the frequency response of the perforant pathway, the major neocortical input to the hippocampus [23], we showed the existence of an activity threshold to elicit a detectable fMRI response. More specifically, we showed that (1) a certain level

of activity, in an approximately constant population of neurons, must be reached in order to start a detectable BOLD signal, (2) the activity-threshold for BOLD elicitation can be reached by applying trains of pulses at relatively low frequencies (4–5 Hz for the perforant path), (3) once the threshold is crossed, the BOLD signal (magnitude and extension of the activation) is linearly correlated with the stimulating current, (4) at current intensities evoking a half-maximal neuronal spiking response, the activity spreads polysynaptically, with increasing stimulation frequencies up to 20 Hz. Thus, stimulation protocols often consisted in 6–10 trains of electrical pulses (100 μs biphasic pulses) repeated every 30–60 s (total duration of the trial 180–600 s) and trials repeated three to five times per condition. The duration of the stimulation train can be adjusted to the specific needs, but durations between 2 and 6 s at frequencies ranging from 4 to 20 Hz produce BOLD responses of excellent amplitude (larger than 4% change) in a variety of preparations [18, 22–25]. Off periods between stimulation trains sufficiently long as to allow a full recovery of the hemodynamic response (25–30 s in rats and mice) increase the SNR of the response and the statistical power of the analysis. A good coordination between image acquisition and timing of stimulus presentation is necessary and easily achievable using the TTL signals generated by the imaging protocols to synchronize the pulse generator (see Fig. 1). Duration of the stimulation train, pulse shape and intensity, frequency, and any other stimulus parameter can be systematically varied for specific purposes [26]. Within each EPI acquisition, it is advisable to acquire long-enough baselines (4–8 volumes) before the first stimulation train that will facilitate posterior quantifications of BOLD signal change.

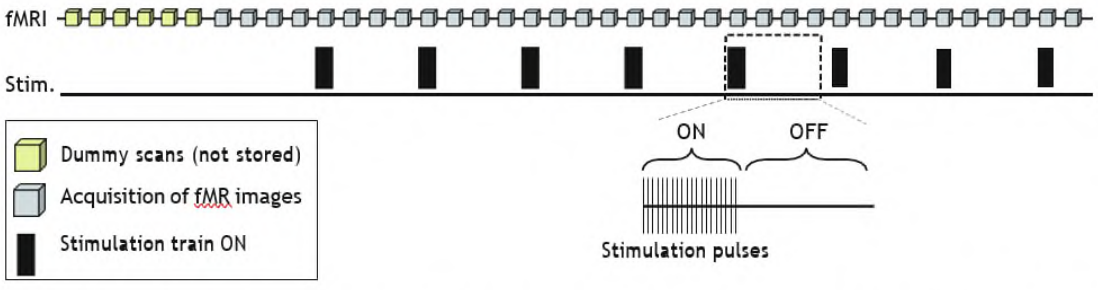

Fig. 1 Scheme representing the image acquisition (up) and the stimulus (down) during the time course of an fMRI experiment. Green squares represent the time for dummy scans at the beginning of the acquisition

3.4 Intracerebral Electrode Implant for fMRI

Most of the BOLD based fMRI experiments are acquired using EPI images, which are very sensitive to T2* changes. Practically speaking, a number of factors can confabulate causing a deterioration of the quality of the functional images. When working with surgically manipulated animals, especially in acute preparations, extreme care has to be taken to minimize bleeding. After the surgery and before cementing the implant to the skull (see below) thorough cleaning of the exposed cranium is mandatory.

In order to improve the SNR, the tip of the electrode is bent (using a burner and some forceps) to form a 90◦ angle, so it could go inside the brain leaving the main body of the pipette outside parallel to the head of the rat, minimizing the implant's height and allowing a closer proximity between the MRI array coil and the head of the animal.

The method described here is based on standard procedures used in electrophysiological experiments with rats adapted to the MRI requirements. Similar protocols are used for mice.

1. Weigh the animal.

2. Dissolve urethane in sterile 0.9% saline. Warm it to room temperature before injection.

3. Place the animal in an induction chamber, and induce anesthesia with 4% isoflurane in 100% oxygen (1 L/min). Wait until the animal is superficially sedated (see Note 9).

4. Inject urethane intraperitoneally (1.3 g/Kg dose for rats and 1.5 g/kg dose for mice, see Note 10). Wait until the total absence of withdrawal reflexes. Induction time is heterogeneous across animals and strains. If after 1 h of the initial dose the animal shows reflexes, additional doses (10–20% of initial dose) can be injected. In our experience, adjustment of the initial dose is necessary for different strains. The slow process of induction of anesthesia ensures a steady-state anesthesia (with stable vital constants) during more than 8 h.

5. Upon induction, place the animal in a heating pad to maintain the animal's body temperature at 37 ◦C. Use a rectal temperature probe with lubricating jelly

to monitor the temperature.

6. Shave the head around the incision area.

7. When the animal reaches an appropriate level of anesthesia, fix the animal's head in a stereotaxic frame.

8. Inject subcutaneous local anesthetic (200 µL Bupivacaine, 0.5%) in the incision points, using a 1 cc syringe with a 20G needle tip.

9. In order to prevent eye damage, employ ophthalmic gel on each eye. The gel needs to be reapplied during the surgery to ensure that eyes are covered at all times.

10. Make an incision (1 cm long) at the top of the head by pressing firmly with a scalpel in an anteroposterior direction. Remove excess skin to expose the skull. Cauterize the skin rims, avoiding burning the skull to prevent image artifacts, and apply hydrogen peroxide to remove any source of bleeding (see Note 11).

11. Calculate the goal stereotaxic coordinates. Modern tools have been developed to facilitate electrode localization [27].

12. Once the target site is located, trephine holes are made using a manual drill. First-time used drill-bits require deep cleaning to remove metal traces that can detach and enter the craniotomy producing large image artifacts.

(a) Carefully rotate the drill bit over the skull until achieving a circular craniotomy (2 mm diameter).

(b) Delicately pinch the dura using a curved 25G needle. For mice, it is better to avoid this step to minimize bleeding. The dura can be broken directly when introducing care- fully the electrode in step 13.

(c) Add saline to the craniotomy once dura is pierced to avoid dryness.

13. Slowly lower the MRI-compatible electrode until it reaches the desired ventral coordinate (see Notes 12 and 13). If the dura is not broken by the electrode in the case of mice, do not force it (the electrode can be broken or the

brain damaged). Go back to step 12(b) and pinch it with the needle.

14. Deeply clean the skull using a dry cotton swab, eliminating any bleeding. Add a small drop of tissue adhesive to seal the tissue, and wait for 10 min.

15. Fix the electrode with several layers of acrylic.

(a) Pay special attention to the first layer of acrylic. This is the critical one and should cover as much surface of the skull, including the electrode, as possible. Use less viscous cement in this first layer than in next ones. Wait until it the layer is completely dry (20 min) before applying more cement.

(b) In mice the first layer is crucial. The skull is smaller com- pared with rats, and the cement has a smaller surface to weld in. Thus, the electrode is more exposed being susceptible of movements and/or breakages. In order to minimize these, we recommend generously covering the section of the electrode closer to the mouse's head using acrylic.

(c) Apply extra layers around the implant until fully embed- ding it, preventing post-surgical movement and protecting it during the transport of the animal to the MRI room. Avoid contact of the cement with the skin during the whole process. This precaution will minimize the probability of bleeding during the imaging session.

16. When the cement is completely dry, remove the electrode holder.

17. Detach the animal from the stereotaxic frame and place it in a transfer cage. In order to avoid temperature dropping, maintain the animal in the heating pad until its transport to the imaging facility.

3.5 fMRI

In order to prevent temperature drop, preheat the magnet's heating system before the animal arrives to the facility.

1. Place the animal on the MRI bed.

2. Check that the correct level of anesthesia has been maintained.

3. Insert the rectal temperature probe using lubricating jelly and tape it in place.

4. Fix the animal's head in an MRI-compatible stereotaxic device.

5. Place the physiological monitoring device (MRI-compatible sensor with foot clip) or the breathing piezoelectric sensor.

6. Cover the exposed skull and the implant with agarose, with special emphasis in filling all the possible empty spaces between the head of the animal and the coil (see Note 14).

7. Connect the electrode to the current source.

8. Using the oscilloscope, cross-check the impedance of the electrode that should match the value obtained during its fabrication, discarding a possible breakdown in the process of implantation or during the accommodation of the animal in the MRI setup.

9. Fix the coil in the MRI bed over the head of the animal, as close as possible to the skull (see Note 15).

10. Place the animal inside the RF coil aligning the approximate center of the brain with the magnet isocenter.

11. Acquire T2-weighted anatomical images in the three orthogonal planes.

12. Even when the animal positioning is accurate, there can be small inter-animal differences when defining an exact position. In order to do grouped analyses, it is interesting to minimize this variability. Thus, we recommend using anatomical land- marks to position EPI slices always in the same orientation. A possible strategy is:

(a) Take the plane that cut the base of cerebellum and the anterior commissure (see Fig. 2a).

(b) Take the midline plane that separates the brain in left and right hemispheres (Fig. 2b, c).

(c) Use the above anatomical planes to define the angle and positioning of the slices for functional imaging. In our case, 15 slices are

positioned perpendicular to the planes with the sixth more anterior slice containing the anterior commissure (Fig. 2d).

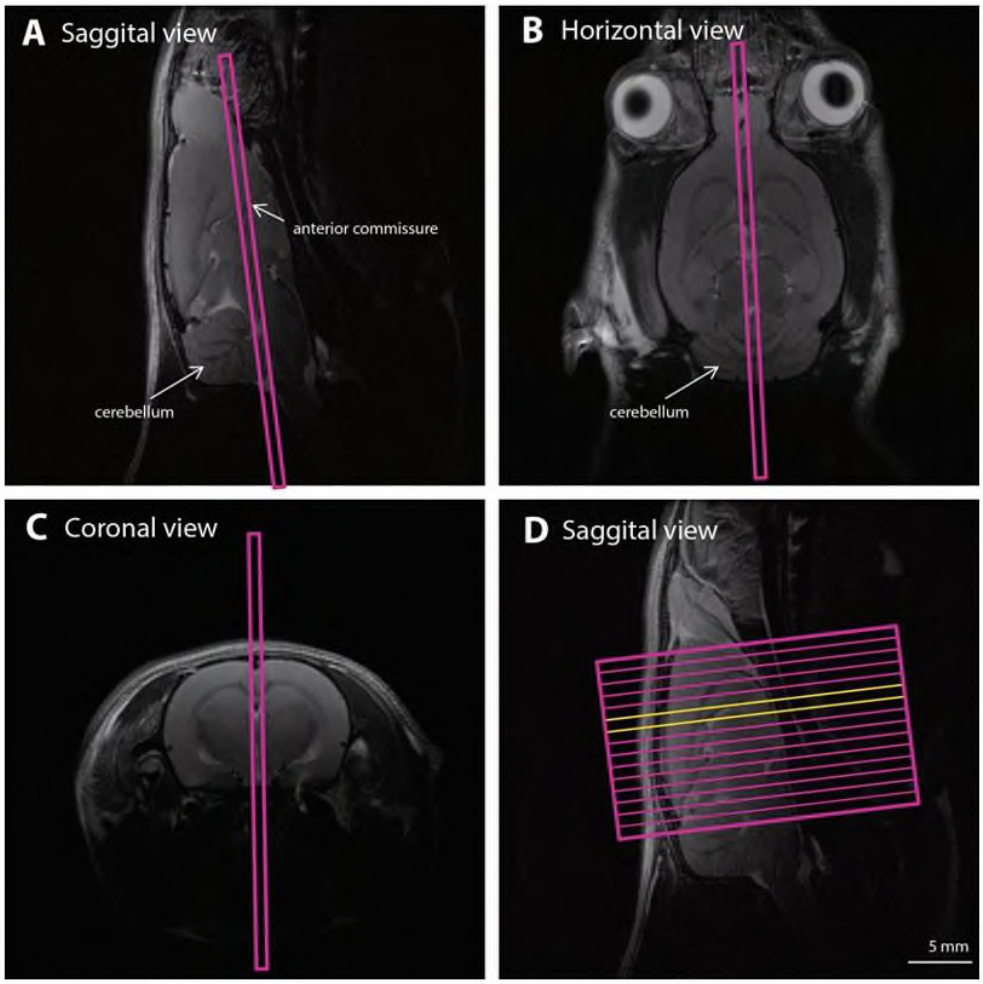

Fig. 2 Position of selected slices using anatomical landmarks. Sagittal image (a) is used to calculate the angle of the plane (pink) defined by the anterior commissure and the base of the cerebellum. Horizontal (b) and coronal (c) images are used to calculate the plane (pink) that goes through the midline. Finally, EPI planes for functional imaging (d) are positioned perpendicular to the anatomical planes calculated previously. To assure a similar anteroposterior location of the EPI images across animals, an anatomical landmark is also used, in our case the sixth most anterior slices is located on the anterior commissure (d, yellow slice)

13. Use a shimming procedure to adjust field homogeneity in the brain. In our case, we use the MapShim macro implemented by Bruker.

14. Adjust the EPI images according to the landmarks mentioned in step 12 (see Note 16) and use saturation slices around the brain. Acquire a set of EPI images without stimulation to check proper image acquisition (no folding, ghosts, etc.)

15. Acquire an anatomical image with the same geometry than the EPI images but higher (at least double) in plane spatial resolution. It will help to identify anatomical landmarks and co-registration of brain templates for grouped analysis.

16. Start data acquisition.

3.6 Data Analysis

The development of either commercial or open-source software tools for fMRI analysis has greatly facilitated the applicability of fMRI and has contributed to its massive widespread. Nevertheless, due to the complex mathematical work behind the generation of brain activation maps, it is important to apply proper and robust statistical methods, e.g., to avoid false positives [28]. For a deep discussion about the analysis see [29, 30]. The workflow for the data analysis used in our laboratory implies linear detrending, temporal (0.015–0.2 Hz) and spatial filtering (3 3 full width at half maximum gaussian kernel of 1.5 sigma) of voxel time series, a general linear model or cross-correlation analysis with a simple boxcar model shifted forward in time (typically by the employed TR), or a boxcar convolved with the hemodynamic response function (HRF). Typical functional maps obtained in one of our electric-stimulation fMRI experiments are shown in Fig. 3.

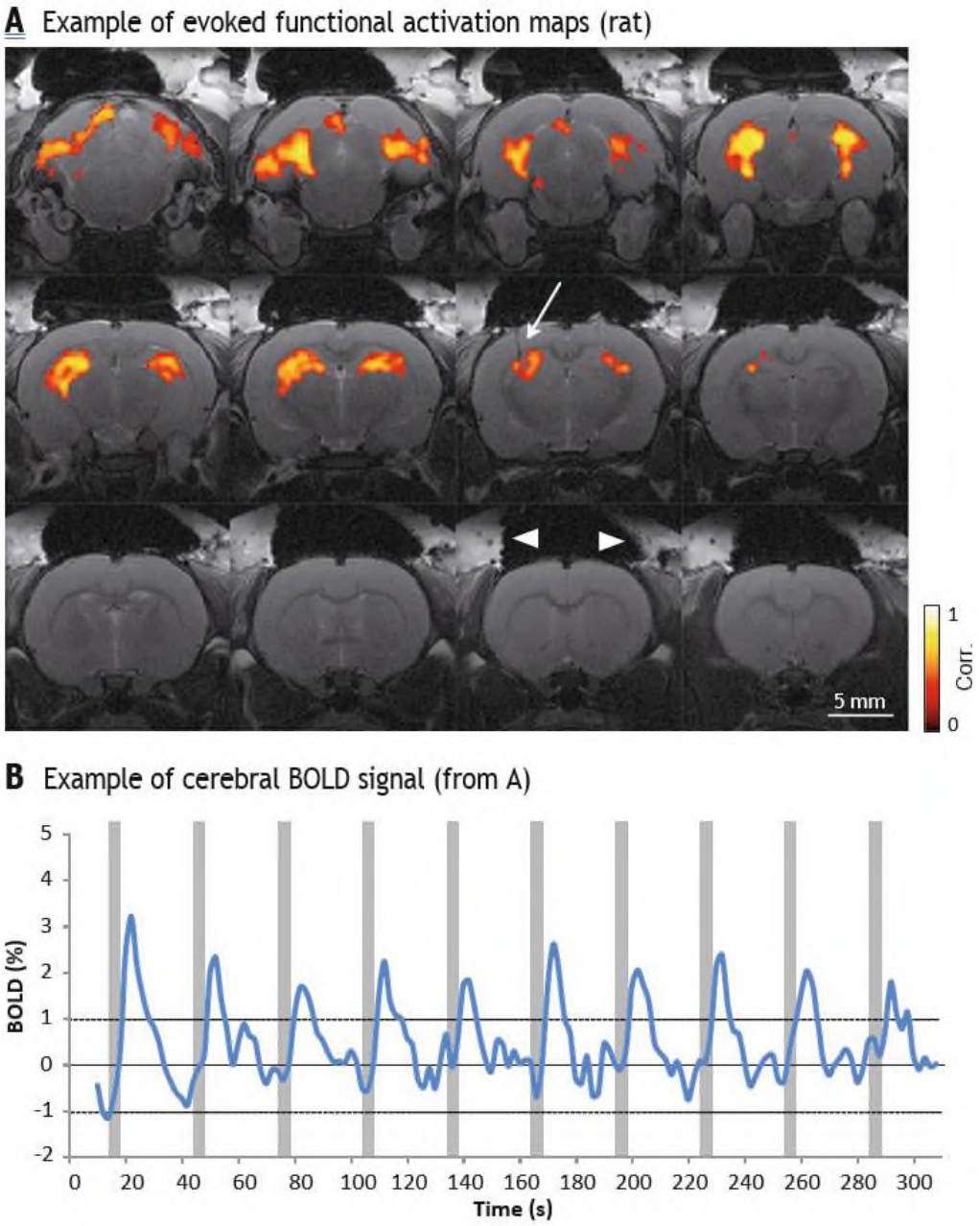

Fig. 3 Brain-wide functional connectivity of dorsal CA3. (a) fMRI BOLD map overlaid on anatomica T_2-weighted images. Color-code denotes the correlation of the BOLD signal with the stimulation protoco convolved with a hemodynamic function (*see* text). The arrow shows the artifact caused by the carbor electrode. Arrowheads show agarose. (b) Global BOLD signal time course of the significantly ($P < 0.001$) activated voxels in response to ten trains of stimulation (indicated by vertical gray bars), delivered at 10 Hz. Graph shows the mean of 3 repetitions of the same protocol

4 Notes

1. Alternatively, breathing rate can be monitoring alone using a simple custom designed piezoelectric device (sensitive to pressure) positioned in the chest of the animal.

2. Usually, water bath is non-MRI compatible, so it has to be positioned outside the 5 Gauss security area. The bath is connected to the water blanket through two 5 m long silicon tubes.

3. The automatic temperature control system is based on the Arduino microcontroller (Arduino MEGA 2560, Arduino S.r. l., Italy). To maintain the physiological temperature of the animal stable automatically, a PID (Proportional-Integral- Derivative) has been developed. The microcontroller obtains, through serial communication (using a RS232 Shield V2, Link- Sprite Technologies, Inc., Longmont, CO), the temperature of the animal from the signal conditioner and it generates a control action that is transmitted to the thermostat to control the temperature of the fluid pumped to the bed. This control system allows automatic temperature control, maintaining almost stable the temperature of the body of the animal being scanned. The technician can interact with the automatic temperature control system through a keypad and a display, being able to set the desired temperature for the animal.

4. Agarose can be prepared in deuterated water, so it will be invisible for MRI. Nevertheless, based on our experience, there are no benefits in terms of fMRI maps acquisition.

5. Sequence parameters for GE-EPI images: field of view (FOV),

25 25 mm; slice thickness, 1 mm; 15 slices; matrix, 96 96; segments, 1; flip angle, 60◦; echo time (TE), 15 ms; repetition time (TR), 2000 ms; and four dummy scans.

6. Alternatively you could use a Spin Echo (SE) sequence with similar parameters. There is extensive literature reviewing the impact of the employed sequence methodology in the obtained fMRI results [6]. Briefly, SE is more specific to microvasculature changes but less sensitive whereas GE is more

influenced by changes in macrovasculature but overall more sensitive.

7. Sequence parameters for RARE images: FOV, 25 × 25 mm; slice thickness, 1 mm; 15 slices; matrix, 192 × 192; RARE factor, 8; effective TE (TEeff), 56 ms; TR, 2000 ms.

8. Small electrode tips will cause less tissue damage during implantation, but the higher electric impedance would require higher voltages to inject a same amount of current and there- fore the possibility to overheat and damage the tissue. Thus, there is a compromise between these two parameters. In our experience, an electrode tip of 200 µm render good stimulation while minimizing tissue damage.

9. Some animal strains are more susceptible to anesthetics mixture and can be affected by the interaction of urethane and isoflurane. In this case, we recommend injecting the animal without previous exposure to other anesthetic.

10. Usually, urethane is injected at doses in the range of 1.2–1.4 g/ Kg for rats and 1.4–1.6 for mice.

11. In our experience, when working with mice, the complete removal of the skin over the skull significantly increases the quality of the fMRI images. To do that, gently cut with surgical scissors the skin over the head. Remove the excess skin, cauterize borders (with extreme caution to avoid overheating the skull) and apply hydrogen peroxide to clean the area. Carefully remove any trace of blood.

12. For instance, to stimulate the CA3 region of the dorsal hippo- campus in the rat the coordinates, referenced to Bregma, are: 3.5 mm anteroposterior and 3.6 mm lateral, initial position; 3.8 mm ventral to the dural surface, based on [31].

13. The same procedure can be followed to insert a recording electrode in the desired area to be sure about stimulation electrode positioning. Nevertheless, care must be taken when placing the recording electrode to minimize brain damage. Ideally, this recording electrode should be placed in a region not fundamental for the fMRI study.

14. EPI images are highly sensible to abrupt changes in magnetic

susceptibility originating artifacts in the border where the variation occurs. Due to the specific configuration used in our set up, when the phase array coil is positioned, there is an empty space between the surface coil and the head of the animal. We fill this space with agarose using a syringe previously filled with agarose 0.5%.

15. Avoid excessive pressure between the coil and electrode. Usually electrodes are fragile and break easily during the experiment if there is some of pressure on them.

16. The employed FOV usually exceeds the cross section of the subject to prevent artifacts from image folding. The slice thick- ness is 1 mm for rats and 0.8 mm for mice, but depending on the SNR and the expected level of activation, it could be decreased.

Acknowledgements

This work was supported by the Spanish Ministerio de Economía y Competitividad (MINECO) and FEDER funds under grants BFU2015-64380-C2-1-R (S.C.) and BFU2015-64380-C2-2-R

(D.M.) and EU Horizon 2020 Program 668863-SyBil-AA grant (S.C.). S.C. acknowledges financial support from the Spanish State Research Agency, through the “Severo Ochoa” Programme for Centres of Excellence in R&D (ref. SEV- 2013-0317).

References

[1] Crosson B, Ford A, McGregor KM, Meinzer M, Cheshkov S, Li X, Walker-Batson- D, Briggs RW (2010) Functional imaging and related techniques: an introduction for rehabil- itation researchers. J Rehabil Res Dev 47(2): vii–xxxiv

[2] Ogawa S, Lee TM, Kay AR, Tank DW (1990) Brain magnetic resonance imaging with con- trast dependent on blood oxygenation. Proc Natl Acad Sci U S A 87(24):9868–9872

[3] Logothetis NK (2008) What we can do and what we cannot do with fMRI. Nature 453 (7197):869–878. https://doi.org/10.1038/ nature06976

[4] Moreno A, Jego P, de la Cruz F, Canals S (2013) Neurophysiological, metabolic and cel- lular compartments that drive neurovascular coupling and neuroimaging signals. Front Neuroenerg 5:3. https://doi.org/10.3389/ fnene.2013.00003

[5] Jego P, Pacheco-Torres J, Araque A, Canals S (2014) Functional MRI in mice lacking IP3-dependent calcium signaling in astrocytes. J Cereb Blood Flow Metab 34 (10):1599–1603. https://doi.org/10.1038/ jcbfm.2014.144

[6] Greve JM (2011) The BOLD effect. Methods Mol Biol 771:153–169. https://doi.org/10. 1007/978-1-61779-219-9_8

[7] Masamoto K, Kanno I (2012) Anesthesia and the quantitative evaluation of neurovascular coupling. J Cereb Blood Flow Metab 32 (7):1233–1247. https://doi.org/10.1038/ jcbfm.2012.50

[8] Khubchandani M, Mallick HN, Jagannathan NR, Mohan Kumar V (2003) Stereotaxic assembly and procedures for simultaneous electrophysiological and MRI study of con- scious rat. Magn Reson Med 49(5):962–967. https://doi.org/10.1002/mrm.10441

[9] King JA, Garelick TS, Brevard ME, Chen W, Messenger TL, Duong TQ,

Ferris CF (2005) Procedure for minimizing stress for fMRI stud- ies in conscious rats. J Neurosci Methods 148 (2):154–160. https://doi.org/10.1016/j. jneumeth.2005.04.011

[10] Ferris CF, Febo M, Luo F, Schmidt K, Brevard M, Harder JA, Kulkarni P, Messenger T, King JA (2006) Functional mag- netic resonance imaging in conscious animals: a new tool in behavioural neuroscience research. J Neuroendocrinol 18(5):307–318. https:// doi.org/10.1111/j.1365-2826.2006.01424. x

[11] Tennant DA, Duran RV, Gottlieb E (2010) Targeting metabolic transformation for cancer therapy. Nat Rev Cancer 10(4):267–277. https://doi.org/10.1038/nrc2817

[12] European Convention for the Protection of vertebrate animals used for experimental and other scientific purposes (2006) Appendix A. Guidelines for accommodation and care of animals (Article 5 of the Convention)

[13] Hendrich KS, Kochanek PM, Melick JA, Schid- ing JK, Statler KD, Williams DS, Marion DW, Ho C (2001) Cerebral perfusion during anes- thesia with fentanyl, isoflurane, or pentobarbi- tal in normal rats studied by arterial spin- labeled MRI. Magn Reson Med 46 (1):202–206

[14] Schroeter A, Schlegel F, Seuwen A, Grandjean J, Rudin M (2014) Specificity of stimulus-evoked fMRI responses in the mouse: the influence of systemic physiological changes associated with innocuous stimulation under four different anesthetics. NeuroImage 94:372–384. https://doi.org/10.1016/j. neuroimage.2014.01.046

[15] Sonnay S, Just N, Duarte JM, Gruetter R (2015) Imaging of prolonged BOLD response in the somatosensory cortex of the rat. NMR Biomed 28(3):414–421. https://doi.org/10. 1002/nbm.3263

[16] Paasonen J, Salo RA, Shatillo A, Forsberg MM, Narvainen J, Huttunen JK, Grohn O (2016) Comparison of seven different anesthesia pro- tocols for nicotine pharmacologic magnetic resonance imaging in rat. Eur Neuropsycho- pharmacol 26(3):518–531. https://doi.org/

10.1016/j.euroneuro.2015.12.034

[17] Maggi CA, Meli A (1986) Suitability of ure- thane anesthesia for physiopharmacological investigations in various systems. Part 2: Cardiovascular system. Experientia 42 (3):292–297

[18] Moreno A, Morris RG, Canals S (2016) Frequency-dependent gating of hippocampal- neocortical interactions. Cereb Cortex 26 (5):2105–2114. https://doi.org/10.1093/ cercor/bhv033

[19] Pawela CP, Biswal BB, Hudetz AG, Schulte ML, Li R, Jones SR, Cho YR, Matloub HS, Hyde JS (2009) A protocol for use of medeto- midine anesthesia in rats for extended studies using task-induced BOLD contrast and resting-state functional connectivity. Neuro- Image 46(4):1137–1147. https://doi.org/ 10.1016/j.neuroimage.2009.03.004

[20] Shyu BC, Lin CY, Sun JJ, Sylantyev S, Chang C (2004) A method for direct thalamic stimula- tion in fMRI studies using a glass-coated car- bon fiber electrode. J Neurosci Methods 137 (1):123–131. https://doi.org/10.1016/j. jneumeth.2004.02.015

[21] Sultan F, Augath M, Murayama Y, Tolias AS, Logothetis N (2011) esfMRI of the upper STS: further evidence for the lack of electrically induced polysynaptic propagation of activity in the neocortex. Magn Reson Imaging 29 (10):1374–1381. https://doi.org/10.1016/j. mri.2011.04.005

[22] Alvarez-Salvado E, Pallares V, Moreno A, Canals S (2014) Functional MRI of long-term potentiation: imaging network plasticity. Philos Trans R Soc Lond Ser B Biol Sci 369 (1633):20130152. https://doi.org/10. 1098/rstb.2013.0152

[23] Canals S, Beyerlein M, Murayama Y, Logothe- tis NK (2008) Electric stimulation fMRI of the perforant pathway to the rat hippocampus. Magn Reson Imaging 26(7):978–986. https://doi.org/10.1016/j.mri.2008.02.018

[24] Godino Mdel C, Romera VG, Sanchez- Tomero JA, Pacheco J, Canals S, Lerma J, Vivancos J, Moro MA, Torres M, Lizasoain I, Sanchez-Prieto J (2013) Amelioration of ische- mic brain damage by peritoneal dialysis. J

Clin Invest 123(10):4359–4363. https://doi.org/ 10.1172/JCI67284

[25] Hadar R, Vengeliene V, Barroeta Hlusicke E, Canals S, Noori HR, Wieske F, Rummel J, Harnack D, Heinz A, Spanagel R, Winter C (2016) Paradoxical augmented relapse in alcohol-dependent rats during deep-brain stimulation in the nucleus accumbens. Transl Psychiatry 6(6):e840. https://doi.org/10. 1038/tp.2016.100

[26] Tehovnik EJ, Tolias AS, Sultan F, Slocum WM, Logothetis NK (2006) Direct and indirect acti- vation of cortical neurons by electrical micro-stimulation. J Neurophysiol 96(2):512–521. https://doi.org/10.1152/jn.00126.2006

[27] Pallares V, Moya J, Samper-Belda FJ, Canals S, Moratal D (2015) Neurosurgery planning in rodents using a magnetic resonance imaging assisted framework to target experimentally defined networks. Comput Methods Prog Biomed 121(2):66–76. https://doi.org/10. 1016/j.cmpb.2015.05.011

[28] Eklund A, Nichols TE, Knutsson H (2016) Cluster failure: why fMRI inferences for spatial extent have inflated false-positive rates. Proc Natl Acad Sci U S A 113(28):7900–7905. https://doi.org/10.1073/pnas.1602413113

[29] Poldrack RA, Mumford JA, Nichols TE (2011) Handbook of functional MRI data analysis. Cambridge University Press, New York

[30] Ashby FG (2011) Statistical analysis of FMRI Data. MIT Press, Cambridge, MA

[31] Paxinos G, Watson C (2007) The rat brain in stereotaxic coordinates. Academic Press, Else- vier, New York